Measurements and analysis of atomic emission from atomic Li, Na, and K seeded in different flames for potential application to temperature sensing

Yuhe Zhang
Supervisor: Zhongshan Li
Co-supervisor: Wubin Weng

Bachelor's Thesis

May, 2017 (Duration: 2 months)

LUND UNIVERSITY

Department of Physics
Combustion Physics Division

Abstract

Alkali metal atoms, especially sodium and potassium, show an intense fluorescence in hot flue gases. The bright fluorescence emitted by alkali metal atoms offers a large potential for spectroscopic combustion analysis. In this thesis, the temperature dependence of the two-component fluorescence intensity ratio Na/K, as well as the three-component ratio $Na \cdot Li/K^2$ was investigated in the flames with known relative concentrations of seeded alkali elements. A theoretical simulation based on thermal radiation excitation was performed to describe the temperature dependence of fluorescence intensity ratios Na/K and $Na \cdot Li/K^2$ in burned gas region. However, measurements show that the two-component fluorescence intensity ratio Na/K is pretty sensitive to the gas temperature whereas the three-component ratio $Na \cdot Li/K^2$ is less temperature dependent. The hot flue gas environment was provided by a modified Perkin-Elmer burner and the alkali metal atoms (Na, K, and Li) were provided through Na_2CO_3, K_2CO_3, and Li_2CO_3 water solution seeding.

Contents

1 Introduction 1
1.1 Background 1
1.2 Outline of this thesis 2
2 Quantitative assessment of alkali fluorescence 2
2.1 Spontaneous emission and Einstein-A coefficient 2
2.2 Population of the excited state 3
2.3 Influence of chemical environment on thermodynamic equilibrium 4
2.4 Line broadening and self-absorption of alkali fluorescence 5
3 Model prediction of alkali fluorescence intensity ratios 6
3.1 The population of the excited state 7
3.2 The mole fraction of atomic alkali metals 8
3.3 Transmitted fraction of the spontaneous emission 9
3.4 Prediction of alkali fluorescence intensity ratios 10
4 Methods 12
4.1 Experimental setup 12
4.2 Preliminary measurements 13
4.3 Fluorescence intensity and temperature measurements 14
5 Results and Discussion 14
5.1 Stability of the system 14
5.2 Fluorescence intensity dependence of the alkali concentration 15
5.3 Temperature dependence of the fluorescence intensity ratio Na/K 16
5.4 Temperature dependence of the fluorescence intensity ratio $\mathbf{Na \cdot Li/K^2}$ ... 18
5.5 Discussion on deficiencies of the method 18
6 Conclusion and Outlook 19
Appendices **23**
Appendix A: Code used in the calculation of self-absorption (Potassium) 23
Appendix B: Photographs of Experimental Setup 25

ABBREVIATIONS

FES - Flame Emission Spectroscopy
AAS - Atomic Absorption Spectroscopy
IC - Internal Combustion
ϕ - Equivalence Ratio
SD - Standard Deviation
SNR - Signal-to-Noise Ratio

1 Introduction

1.1 Background

When alkali metals especially sodium and potassium are contained in fuel additives, bright fluorescence is emitted in the burned gas zone by the alkali metal atoms. This fluorescence offers a great deal of flame-related information which is indispensable for understanding the complicated physical and chemical processes involved. A simple, versatile and efficient method to quantitatively study these physical and chemical processes is analytical flame spectroscopy. The alkali metal solution is nebulized into the flame in which the solute and solvent are vaporized and decomposed.

Various researches have been delivered to investigate the bright natural fluorescence of alkali metal atoms in flames. Withrow et al. [1] and Rassweiller et al. [2] obtained the temperature of hot flue gas using the sodium-line reversal method with sodium chloride (NaCl) mist fuel additives to better visualize the flaming process in internal combustion (IC) engines. Reissing et al. [3] and Beck et al. [4] firstly measured the temperature of the burned gas region using the fluorescence intensity ratios of sodium and potassium. In their work, the sodium and potassium fluorescence intensity ratio were regarded as only affected by the excited states population of the sodium and potassium atoms. The influences of the self-absorption of the emitted light and the chemical equilibrium between the sodium and potassium atoms and their oxidation products were not taken into consideration. Mosburger et al. [5, 6, 7] added lithium as a third alkali component to develop the Na-/K-based temperature measurement tool and concluded that the three-component fluorescence intensity ratio $\frac{\mathrm{Li}\cdot\mathrm{Na}}{K^2}$ is only relevant to the temperature of the burned gas region when the concentration of the alkali metals is known. This offers a huge potential for temperature measurement by spectroscopic combustion analysis. The fraction of the self-absorption of the fluorescence light is quantitatively calculated in their work. As a result, their temperature-measurement method was practicable within the accuracy uncertainty of $\pm$100 K.

In this thesis, the temperature dependence of the fluorescence intensity ratios is investigated based on previous researches by Flame Emission Spectroscopy (FES) under an atmosphere with the temperature about 1600K. The influence of the solution concentration is discussed as well as the operating conditions and ranges of this temperature-measurement method. The self-absorption of the fluorescence light is also calculated using the Mathematica code given by Mosburger et al. Since the combustion processes are performed on a burner other than internal combustion engines as used in their research, the code is modified to suit the burner environment. However, although the concentration of the alkali metal solutions is given, the accurate concentration of the atomic Na, Li, and K in the hot gases is not measured. Besides, as discussed in the Outlook chapter, the measurement of the concentration of atomic Na, Li and K can be used to achieve a more accurate temperature measurement than the previous work.

1.2 Outline of this thesis

The thesis starts with a theory chapter, Chapter 2, which describes the quantitative assessment of alkali fluorescence. The model prediction of alkali fluorescence intensity ratios is presented in Chapter 3. The Experiment chapter, Chapter 4, offers a description of the equipment and different measurement techniques used during the project. The results are presented and discussed in Chapter 5. The Conclusion and Outlook chapters provide the main conclusions and a brief discussion of the outlook of the thesis. The code used in the calculation of self-absorption and some photographs of the experimental setup can be found in Appendix A and B.

2 Quantitative assessment of alkali fluorescence

2.1 Spontaneous emission and Einstein-A coefficient

When a quantum mechanical system (such as an atom, molecule or subatomic particle) is in an excited energy state where the life time is limited, it will spontaneously relax to a lower energy state and emit a quantum in the form of a photon with frequency corresponding to the energy difference. This process is called spontaneous emission. The spontaneous emission from alkali metal atoms in the flame environment is called fluorescence because the excitation is affected by the absorption of radiation. Spontaneous emission forms the underlying physics for the spectroscopic measurement and observations conducted in this project. The intensity of the fluorescence depends largely on a constant which is the so-called Einstein-A coefficient.

If the number of the excited state atoms at time *t* is given by $N(t)$, the rate at which transitions occur is:

$$\frac{\partial N(t)}{\partial t} = -A \cdot N(t) \tag{2-1}$$

where A is the rate of spontaneous emission which is also referred to as the Einstein-A coefficient. The Einstein-A coefficient is determined by the overlap of wave functions under the influence of the emitted photon as well as the magnitude of the energy split. It can be calculated by an expression derived by Bransden and Joachain [8] if the accurate expressions for the wave functions of the excited and the lower energy state are known. However, this is almost impossible for non-hydrogen atoms. But the Einstein-A coefficient can be obtained by experimentally measurements of the radiative lifetime of the excited state.

Equation 2-1 can be solved to give:

$$N(t) = N(0)e^{-A \cdot t} = N(0)e^{-\Gamma \cdot t} \tag{2-2}$$

where $N(0)$ is the initial number of the atoms in the excited state and Γ is the radiative decay rate of the transition which is inversely proportional to the excited state lifetime τ. The number of the atoms in the excited states $N(t)$ is seen to decay exponentially with time from Equation 2-2. Therefore, the Einstein-A coefficient also equals to the inverse of the excited state lifetime which can be measured from experiments.

For most atoms, the population of the ground state in the flame environment is by many orders of magnitude higher than that of the higher energy levels. Therefore, the most used transitions for the fluorescence measurements are the transitions occur to or from the ground level, and in particular, the transitions occur from the lowest excited state to the ground state. Correspondingly, the mostly used lines are the resonance lines, and in particular first resonance lines.

As for the alkali fluorescence in the burned gas region, the interested energy states involved in the spontaneous emission are the two lowest excited states and the ground state. Different alkali metal atoms have a various color of fluorescence in the flame due to the different energy separation between the excited state and the ground state. The spectroscopic properties of lithium (Li), sodium (Na), potassium (K), rubidium (Rb) and cesium (Cs) fluorescence are shown in Table 1. The ground state and the excited state are denoted by "p" and "q", respectively. Due to the fine structure energy splitting of the p-orbital, alkali metal atoms usually show two lines in their emission spectrum.

Table 1: Spectroscopic properties of alkali metal fluorescence [9]

	Transition [Notation nl_j]	Degeneracy $g_q - g_p$	Wavenumber $\tilde{\nu}_q$ - $\tilde{\nu}_p$ [cm^{-1}]	Wavelength in air [nm]	Einstein-A coefficient [10^7 1/s]
Li	$2p_{3/2} - 2s_{1/2}$	4 – 2	14904.00 – 0	670.78	3.69
	$2p_{1/2} - 2s_{1/2}$	2 – 2	14903.66 – 0	670.79	3.69
Na	$3p_{3/2} - 3s_{1/2}$	4 – 2	16973.37 – 0	589.00	6.16
	$3p_{1/2} - 3s_{1/2}$	2 – 2	16956.17 – 0	589.59	6.14
K	$4p_{3/2} - 4s_{1/2}$	4 – 2	13042.90 – 0	766.49	3.80
	$4p_{1/2} - 4s_{1/2}$	2 – 2	12985.19 – 0	769.90	3.75
Rb	$5p_{3/2} - 5s_{1/2}$	4 – 2	12816.55 – 0	780.03	3.81
	$5p_{1/2} - 5s_{1/2}$	2 – 2	12578.95 – 0	794.76	3.61
Cs	$6p_{3/2} - 6s_{1/2}$	4 – 2	11732.31 – 0	852.11	3.28
	$6p_{1/2} - 6s_{1/2}$	2 – 2	11178.27 – 0	894.35	2.86

2.2 Population of the excited state

The speeds of gaseous particles in idealized gases are described by Maxwell–Boltzmann distribution as a function of the gas temperature when the system of particles is assumed to have reached thermodynamic equilibrium, as shown in Equation 2-3.

$$f(v) = \sqrt{(\frac{m}{2\pi kT})^3} 4\pi v^2 e^{-\frac{mv^2}{2kT}} \tag{2-3}$$

where v is the velocity, m is the particle mass, and kT is the product of Boltzmann's constant and thermodynamic temperature. Atoms in the flame temperature collide with each other frequently leading to the energy transition among collision atoms. Most of the collisions are elastic, where the collision partners conserve the total kinetic energy. These collisions can also be inelastic, where the kinetic energy is transformed into internal energy or potential energy and vice versa. The Boltzmann distribution law describes the population of the quantized energy states:

$$f(E_i) = \frac{g_i e^{-\frac{E_i}{kTe}}}{Z(T)} \tag{2-4}$$

where *Z(T)* is the partition function of the system which depends only on temperature, g_i denotes the degeneracy of the eigenstate i, T_e is the excitation temperature, and E_i is the eigenvalue of the potential energy.

The gas temperature will be equal to the excitation temperature if thermal equilibrium can be assumed for hot alkali metal atoms in the flame environment. Generally, alkali metal atoms at high temperature can get excited through collisions and undergo relaxation both through quenching and spontaneous emission of light. Due to the lack of irradiation, the rate of relaxation is a little higher than the excitation rate, and the excitation temperature is thus lower than the gas temperature because of the under-population. Nonetheless, the rate of radiative energy loss can be neglected, and thermal equilibrium can be assumed in the flame environment doped with alkali metals in which the collisional excitation and relaxation are considered occurring on a much faster time scale than the radiative relaxation [6,7]. In this state of approximate thermal equilibrium, it is valid to expect the gas temperature is the same as the excitation temperature as defined in the Maxwell–Boltzmann distribution and describe the distribution of the excited states by the Boltzmann distribution law.

Some studies have been conducted to investigate whether the Boltzmann law can be applied to measure the gas temperature via alkali metal fluorescence, and it turns out that at atmospheric pressure, the excitation temperature equals to the gas temperature within an error of 8 K at 2,200 K and the Boltzmann distribution law can be applied to describe the population of the excited state versus the ground state as a function of gas temperature [10-13] :

$$\frac{N_q}{N} = \frac{g_q \cdot e^{-\frac{E_q - E_p}{kT}}}{Z(T)} \tag{2-5}$$

2.3 Influence of the chemical environment on thermodynamic equilibrium

The emitted light is also directly proportional to the number density of alkali metals that are in elemental form in hot flue gases. Chemical reactions have to be considered in the flame environment, by which part of the alkali metals are converted into oxidation products especially hydroxides and no more light will be emitted with the atomic transition wavelength. According to previous researches, it is reasonable to assume chemical and thermodynamic equilibrium under the high-temperature and high-pressure conditions in the hot flue gases of the flame environment [14-17].

One more parameter should be mentioned here, that is the equivalence ratio, Φ. A few properties involved in combustion processes strongly depend on the stoichiometry of the combustion mixture. The equivalence ratio, which is defined as the ratio of the actual fuel/oxidizer ratio to the stoichiometric fuel/oxidizer ratio, is most frequently used to describe the stoichiometry of the mixture.

The chemical equilibria of all alkali elements depend strongly on temperature, equivalence ratio, and pressure. For a given operating condition, the number density of atomic alkali metals can thus be calculated by the software Chemkin-Pro [18]. Chemkin-pro is a combustion simulation software specifically designed for large chemical kinetics simulations which require complex reaction mechanisms. It will automatically calculate component concentration when the initial flame pressure, temperature and reactant concentration are known.

Some irrespective alkali species are also considered in the calculations such as A^-, AO, AO_2, and AH, where the letter A stands for alkali elements. The influence of these species was found to be slight, and hence can be neglected in the calculations.

2.4 Line broadening and self-absorption of alkali fluorescence

Considering that more than 99% of the alkali metal atoms in burned gas region are in the ground state, a large amount of the emitted light can get re-absorbed. Therefore, it is important to take the fraction of reabsorbed light into consideration when calculating the fluorescence intensity ratio.

Boers et al. [19] observed a propane-air flame seeded with sodium chloride (NaCl) at an atmosphere pressure and obtained the total inelastic collision cross section ($\sigma_{c,inel}$) of 24Å^2. The inelastic collision rate can be calculated from the inelastic collision cross section by:

$$Q_{c,inel} = N \cdot \sigma_{c,inel} \cdot \sqrt{\frac{8kT}{\pi\mu}} \tag{2-6}$$

where $Q_{c,inel}$ is the inelastic collisional energy transfer rate, N is the total number of gas molecules per unit volume and μ is the reduced mass of alkali metal atom and collision partner.

Comparing the collisional relaxation rate to the radiative relaxation rate, which is Einstein-A coefficient, the fluorescence quantum yield can be calculated to be 0.04. Due to the small ratio of the radiation to the overall energy transfer rate, it is reasonable to consider all light that gets reabsorbed to be lost, and no more re-emission will be calculated. The fraction of the absorbed light can be calculated by the Beer–Lambert law, in which the line broadening of alkali fluorescence is given by the book Metal Vapor in Flames [20]. The software 'Wolfram Mathematica 9' [21] was used to calculate the fraction of the absorbed light. The code used is given in Appendix A.

The fraction of the reabsorbed light can be calculated by the Beer-Lambert law:

$$Abs = \frac{I_0 - I_T}{I_0} = \frac{\int_{\upsilon=0}^{\infty}\int_{l'=0}^{l} E_\upsilon dl' d\upsilon - \int_{\upsilon=0}^{\infty}\int_{l'=0}^{l} E_\upsilon e^{-\kappa(\upsilon)\cdot n\cdot l'} dl' d\upsilon}{\int_{\upsilon=0}^{\infty}\int_{l'=0}^{l} E_\upsilon dl' d\upsilon} \tag{2-7}$$

where Abs is the fraction of the reabsorbed light, I_0 is the emitted intensity of light, I_T is the intensity of transmitted light, E_υ the spectral distribution of light energy with the light

frequency υ. The absorptivity of the spectral is given by $\kappa(\upsilon)$, the number density of absorbing atoms is given by n and l is the thickness of the hot flue gases. The spectral distribution of the emitting atom spectrum can be regarded as identical to the absorption spectrum of the absorbing atom in the case of self-absorption. The spectral distribution of light energy can thus be expressed by

$$E_\upsilon = c \cdot S(\upsilon) \tag{2-8}$$

where $S(\upsilon)$ is the normalized spectral emission and absorption profile and c is a constant. The absorptivity of the spectral $\kappa(\upsilon)$ can be expressed as:

$$\kappa(\upsilon) = 2.65 \times 10^{-2} \times S(\upsilon) \times f_{pq} \tag{2-9}$$

where f_{pq} is the strength of the oscillator transitioned between the excited state and the ground state.

$$f_q = 1.5 \cdot A \cdot g_p \cdot \lambda^2 \tag{2-10}$$

The normalized absorption profile $S(\upsilon)$ is determined by the line broadening of the spectrum including the natural line broadening, collision line broadening and Doppler line broadening. The width of those broadened transition lines in the frequency domain, $\delta\upsilon_N, \delta\upsilon_C, \delta\upsilon_D$, respectively, can be calculated by Equation 2-11.

$$\delta\upsilon_N = \frac{A}{2\pi}, \delta\upsilon_C = \frac{Q_{c,eff}}{2\pi}, \delta\upsilon_D = 2\sqrt{2ln2 \cdot \frac{kT}{m}} \cdot \frac{\upsilon_0}{c} \tag{2-11}$$

in which $Q_{c,eff}$ is the effective collision rate as can be calculated using the effective cross section and Equation 2-6, kT is the product of Boltzmann's constant and thermodynamic temperature, υ_0 is the center transition frequency of the alkali atom, m the mass of the atom and *c* the speed of light in vacuum.

The effects of these three spectral line broadenings are combined in the Voigt line profile as described by Alkemade et al. as:

$$S_V(\upsilon) = \frac{2\sqrt{ln2}}{\pi\sqrt{\pi}} \cdot \frac{a}{\delta\upsilon_D} \cdot \int_{-\infty}^{\infty} \frac{e^{-y^2} dy}{a^2 + (v-y)^2} \tag{2-12}$$

The parameters a and v with dimension one are defined by

$$a \equiv \sqrt{ln2} \frac{\delta\upsilon_L}{\delta\upsilon_D}, \tag{2-13}$$

$$v \equiv (\upsilon - \upsilon_0) \frac{2\sqrt{ln2}}{\delta\upsilon_D} \tag{2-14}$$

3 Model prediction of alkali fluorescence intensity ratios

As discussed in Chapter 2, the fluorescence intensity can be assumed as mainly influenced by the following factors if the excitation from chemical reactions can be neglected in a certain operating condition: the excited state population, the number of atomic alkali metal atoms in the flame, self-absorption of the emitted light and Einstein transition probability. Under such condition, the fluorescence intensity ratio can be predicted as shown in Equation 3-1 for the case of sodium and potassium.

$$\frac{I_{Na}}{I_K} = \frac{A_{Na}}{A_K} \cdot \frac{n_{Na}}{n_K} \cdot \frac{Tr_{Na}}{Tr_K} \cdot e^{\frac{E_{Na}-E_K}{kT}} \quad (3\text{-}1)$$

The gas temperature, pressure, equivalence ratio and the alkali metal fraction in the fuel are needed for the calculation of the number density of atomic alkali metal atoms n. On the other hand, the number density of alkali metal atoms, temperature, and pressure are needed for the calculation of transmitted light fraction Tr.

As a result, a predicted database of expected fluorescence intensity ratios as a function of pressure, temperature and equivalence ratio at a given concentration of alkali solution can be built. Hopefully, the measured fluorescence intensity ratios can be compared to the database and obtained the temperature information of the flame.

3.1 The population of the excited state

As shown in Equation 2-5, the population of the excited state of alkali metal atoms can be calculated by the Boltzmann distribution law as a function of the gas temperature. The partition function *Z(T)* in the equation is approximately 1 in the temperature interested ranged from 1500K to 2000K. The intensity of spontaneous emission is directly proportional to the population of the excited state. Thus an exponential dependence of the emitted light intensity to the hot-flue gas temperature can be expected as shown in Figure 1.

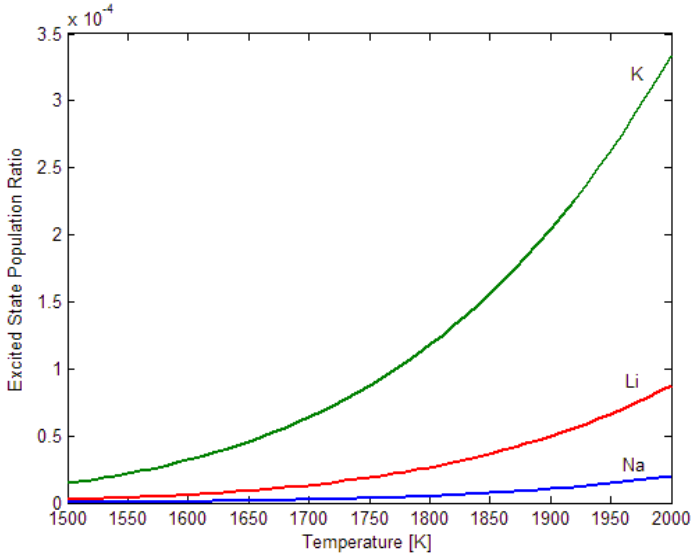

Figure 1: The temperature dependent population of the lowest lying excited state of alkali metals.

The intensity ratio of the measured alkali metal fluorescence is given in Figure 2.

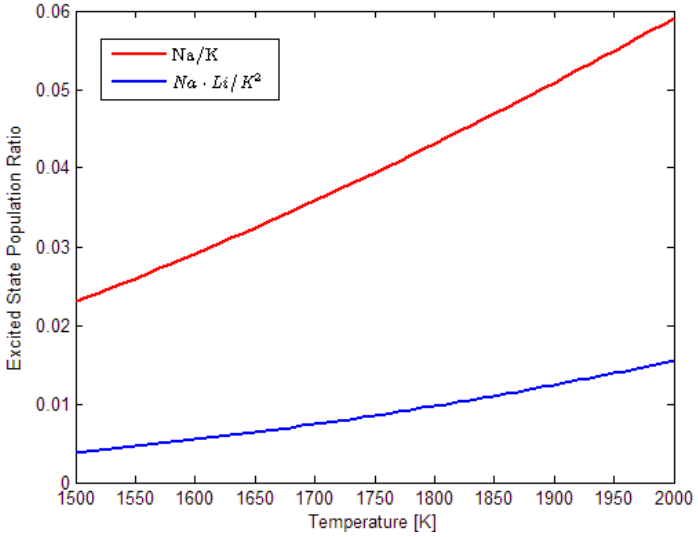

Figure 2: Temperature dependence of the ratio of the excited state populations Na/K and Na Li/K^2.

3.2 The mole fraction of atomic alkali metals

The fraction of atomic Na and K in hot flue gases calculated by Chemikin-Pro as a function of temperature at nearly stoichiometric ratio is shown in Figure 3 in which chemical equilibrium is assumed with the oxidation products of the alkali metal atoms. The fractions of sodium and potassium in the fuel are both set to 50 ppm, which corresponds to the operating condition with 0.005mol/L as will be discussed in the following chapter. The fraction of atomic lithium is not calculated due to the lack of appropriate thermodynamic data that can be used for Chemikin-Pro.

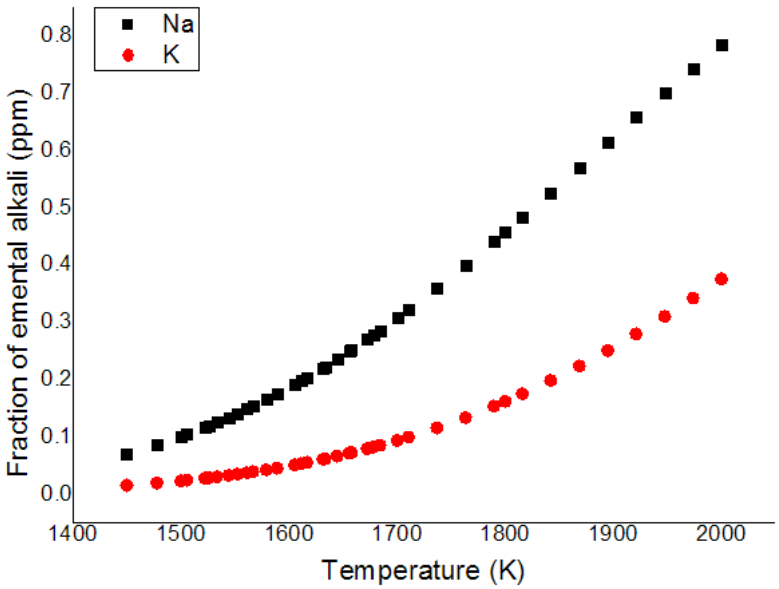

Figure 3: The calculated mole fraction of alkali metal atoms in hot flue gases as a function of temperature (P=1bar, ϕ =0.96).

3.3 Transmitted fraction of the spontaneous emission

The fraction of self-absorption was calculated for a modified Perkin-Elmer burner that was used in the lab with the maximum absorption length of 23mm. The number density of atomic alkali metals is calculated by the product of the number density of molecules given by the ideal gas law and the mole fraction of atomic alkali metals.

Figure 4 shows the fraction of the transmitted light of lithium, sodium, and potassium as a function of temperature at 1ppm atomic mole fraction. Figure 5 shows the influence of atomic mole fractions to the transmitted sodium fluorescence fraction which is supposed to be an exponential dependence as expected from the Beer-Lambert law. According to Figure 4 and 5, more than 85% of the emitted light gets reabsorbed if the mole fraction of the atomic alkali metal is higher than 5 ppm, whereas it can be predicted most emission gets transmitted when the atomic mole fraction is lower than 1 ppm.

The temperature dependence of the ratio of transmitted fluorescence light Na/K and Na Łi/K^2 for a range of atomic mole fractions are shown in Figure 6. Comparing to Figure 5, the temperature dependence of transmitted ratios is much weaker than that of a certain alkali species. The transmitted Na/K ratio is hardly affected by the atomic mole fraction as well as the gas temperature, while the ratio of Na Łi/K^2 does depend on the mole fraction of atomic alkali metals but is almost independent of the temperature.

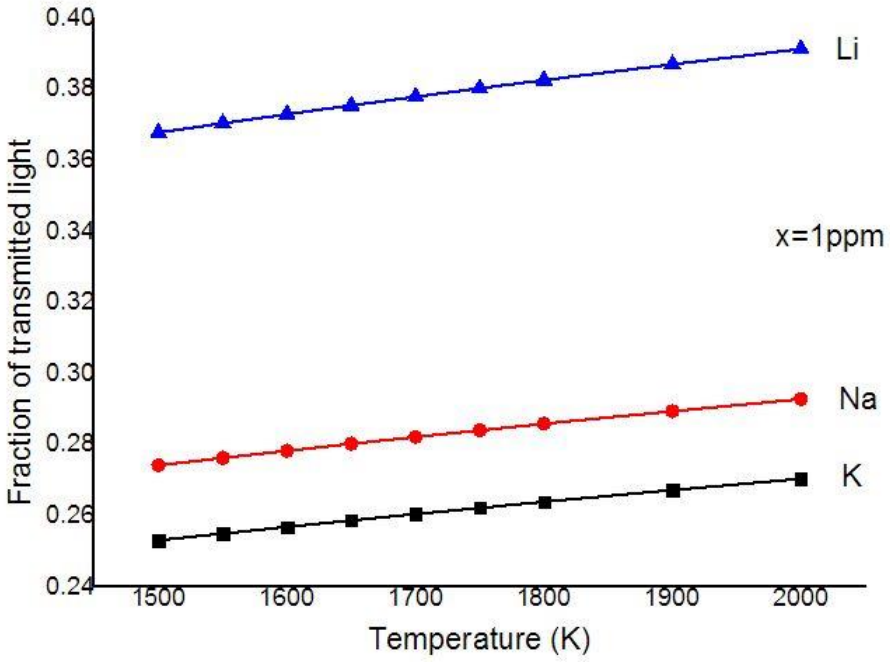

Figure 4: The fraction of transmitted light as a function of temperature (x=1ppm, P = 1bar).

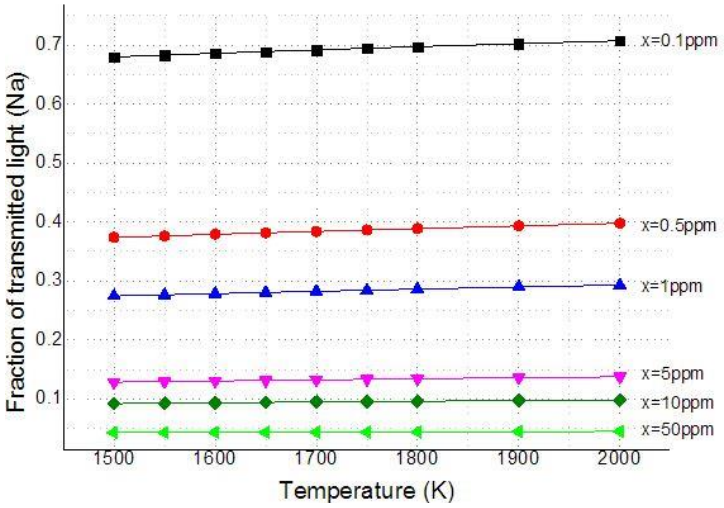

Figure 6: The fraction of transmitted light as a function of temperature for an interested range of atomic mole fractions (P=1 bar).

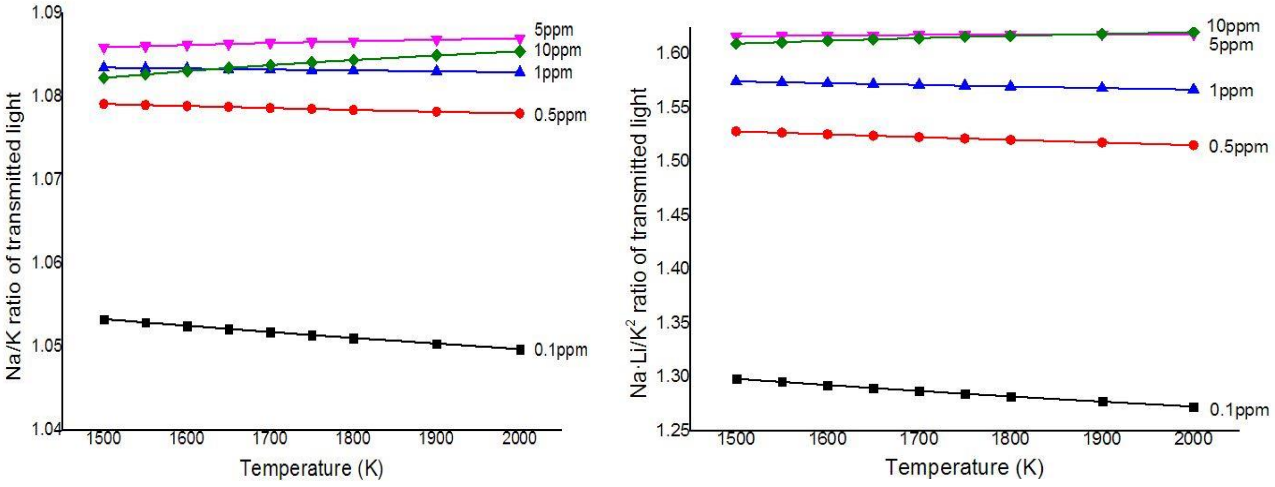

Figure 5: The ratio of the transmitted fluorescence light (a) Na/K and (b) Na·Li/K^2 as a function of temperature for an interested range of atomic mole fractions (P = 1 bar).

3.4 Prediction of alkali fluorescence intensity ratios

Combining the affection of excited state population, atomic mole fraction, self-absorption, and Einstein-A coefficient, one can get the prediction of fluorescence intensity ratios at certain working conditions. Figure 7 is the simulation for one of the experimental condition where the alkali fraction in the fuel is 50 ppm (0.005mol/L), the equivalence ratio equals to 0.96, and an atmosphere pressure. Figure 8 shows the concentration dependence of the predicted Na/K fluorescence ratio at 1700K, nearly stoichiometric ratio in semi-log plot. The fluorescence ratio is shown to depend slightly on the gas temperature and the concentration of alkali solution.

Unfortunately, the fluorescence intensity ratio Na Li/K[2] is not predicted because of the unavailable atomic mole fraction data as mentioned. However, according to the research conducted on IC engines by Mosburger et al. [6, 7], the Na Li/K[2] ratio is nearly unaffected by the equivalence ratio ranged from 0.5 to 2.0 and pressure from 4bar to 10 bar but shows a strong dependence on temperature. The predicted Na Li/K[2] ratio show a monotonic notching increasing dependence of the temperature. Thus it can be used as a direct temperature marker in a certain temperature range in the burned gas region.

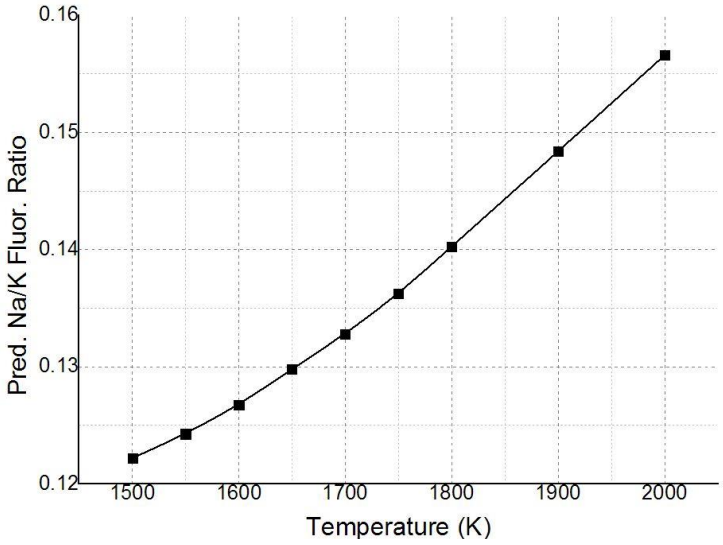

Figure 8: Predicted temperature dependence of Na/K fluorescence intensity ratio (P=1 bar, ϕ =0.96).

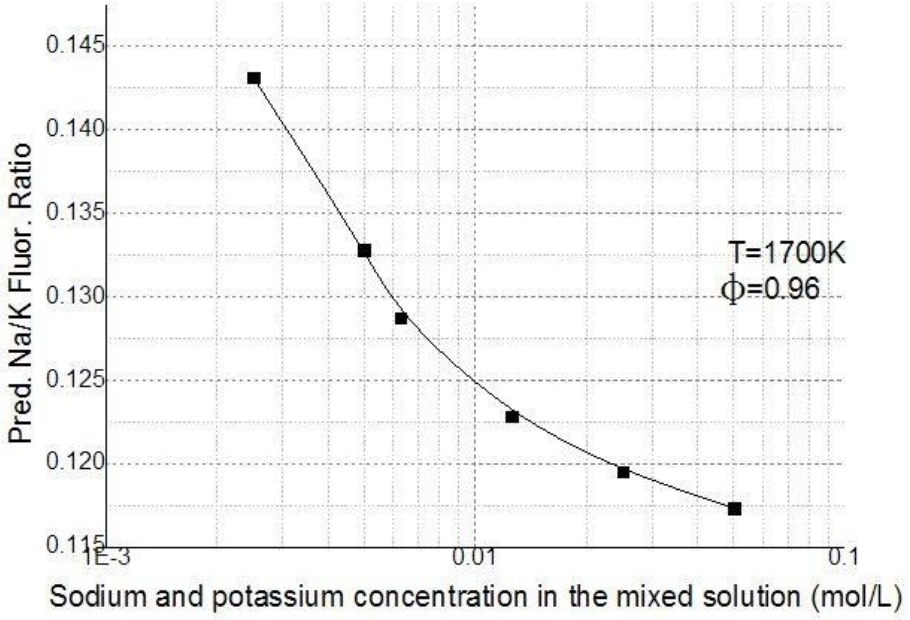

Figure 7: Predicted Na/K fluorescence intensity ratio as a function of alkali concentration in semi-log graph (1700K, ϕ =0.96).

4 Methods

4.1 Experimental setup

The experiment was conducted in the *Enoch Thulin Laboratory*, Lund University. The experimental setup is shown in Figure 9.

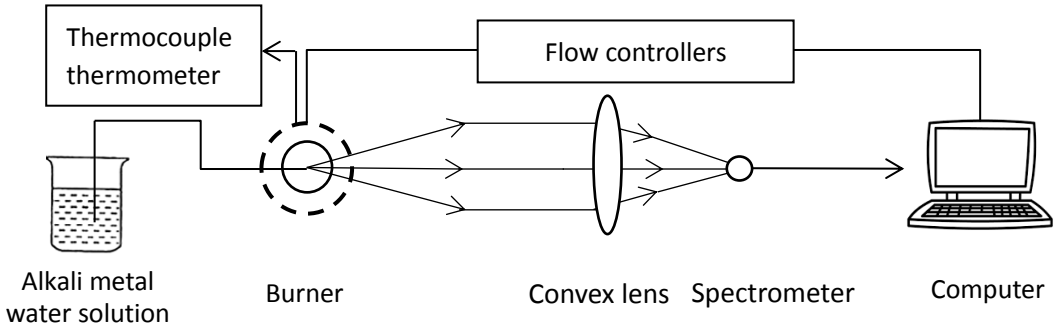

Figure 9: The experimental setup.

The burner used during the emission spectroscopy measurements is a modified water-cooled Perkin-Elmer burner which has an advanced seeding system. The seeding system was used to seed solutions of alkali metals into CH_4-air flames. The burner, as shown in Figure 10, consists of an end cap, a spray chamber, and a water-cooled burner head topped by a circular mesh with an inner and an outer compartment for the co-flow and the premixed fuel blend. A ventilation system was setup above the burner for the secure reason which is not shown in the figure above. The maximum absorption length of this burner is 23mm.

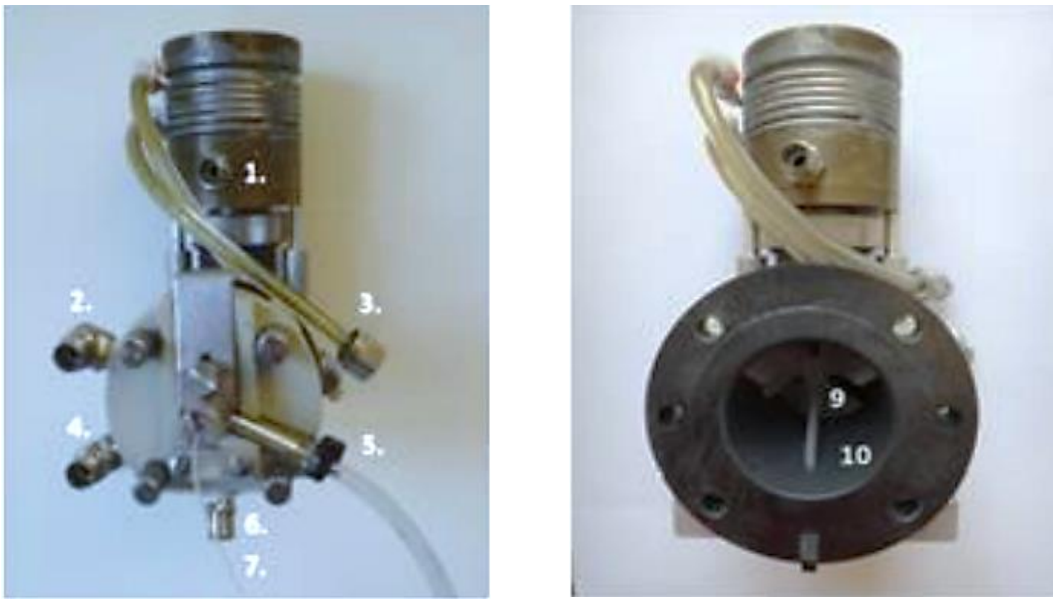

(a) (b)

Figure 10: Photo of the modified Perkin-Elmer burner [22]. (a) With endcap: 1.N_2 co-flow; 2.Auxiliary air; 3.Cooling water; 4.Fuel; 5.Nebulizer air; 6.Drain; 7.Seeding capillary. (b) Endcap removed: 9.Flow spoiler; 10.Spray chamber.

The gas supply for the burner was controlled by Bronkhorst mass flow controllers as shown in Figure 11. The CH_4 and air flows are around 0.5 L/min and 5 L/min, respectively. A stabilizing co-flow of N_2 is set to 10 L/min. The alkali metal water solutions used during the experiments were lithium carbonate (Li_2CO_3), sodium carbonate (Na_2CO_3) and potassium carbonate (K_2CO_3) water solutions. They were seeded with the combustion air by suction through a capillary tube connected to the air inlet at the nebulizer.

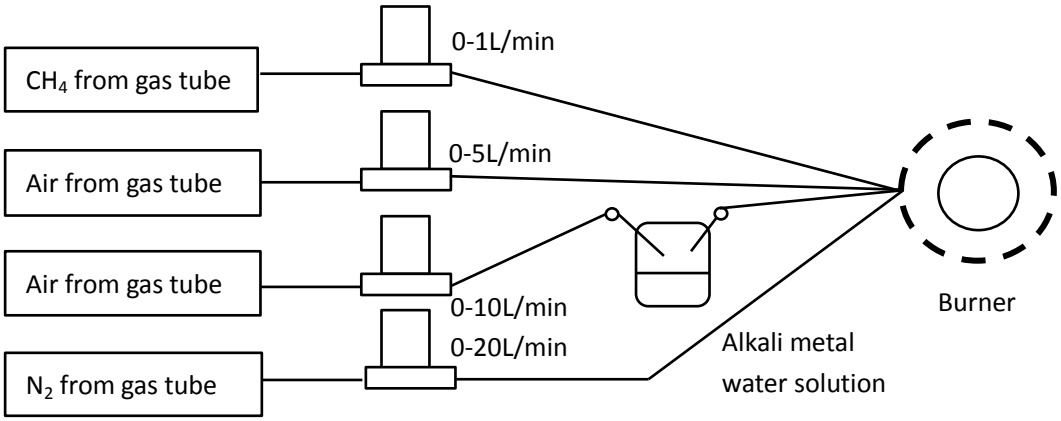

Figure 11: Schematic of the gas-flow arrangement.

The spectrometer used in the lab was a USB2000+ spectrometer made by the Ocean Optics company. The spectral acquisition time was set to 10ms, and each final spectrum was acquired by the average of 10000 measurements. The background spectra were measured using water seeding at the end of each experiment. The spectra were analyzed by the software OriginPro 9 [23]. The end point straight line was used as the baseline when integrating the area of the signal peak.

4.2 Preliminary measurements

Different operating conditions of the burner were tested before the temperature measurement to find the appropriate flame environment. The final working conditions with different equivalence ratio chose for the fluorescence signal measurements are shown in the table below. The stabilizing co-flow of N_2 is set to 5 L/min during the whole process.

Table 2: Working conditions used in the temperature measurements

ϕ	CH_4 (L/min)	Air (L/min)	Air seeding (L/min)
0.85	0.418	1.675	3
0.96	0.464	1.625	3
1.04	0.500	1.59	3
1.14	0.545	1.545	3
1.23	0.582	1.51	3

The fluorescence intensity dependence of the alkali solution concentration was measured to obtain the appropriate range of concentration for the following measurements. The stability of the flame was also tested to assure the effectiveness of the data measured.

4.3 Fluorescence intensity and temperature measurements

The fluorescence signal intensities were measured under various solution concentrations and different equivalence ratio to calculate the two-component fluorescence intensity ratio Na/K as well as the three-component ratio $\mathrm{Na} \cdot \mathrm{Li}/\mathrm{K}^2$. The relationship between the alkali fluorescence intensity ratios and the equivalence ratio or the solution concentration can thus be obtained. The temperatures of the burned gas region were roughly detected by a thermocouple thermometer. As a result, the temperature dependence of the fluorescence intensity ratios can be given. The mass of seeded alkali solutions were measured by calculating the mass difference of the seeding beaker and the leakage bottle.

Several concentrations of alkali metal solutions were chosen after preliminary measurements to be used for the following measurements, as given in Table 3.

Table 3: Solution concentrations used in the intensity measurements

	Li(mol/L)	Na(mol/L)	K(mol/L)
1	0.18	0.05	0.05
2	0.09	0.025	0.025
3	0.045	0.0125	0.0125
4	0.018	0.005	0.005
5	0.009	0.0025	0.0025
6	0.045	0.00625	0.00625
7	0.032	0.005	0.005

5 Results and Discussion

5.1 Stability of the system

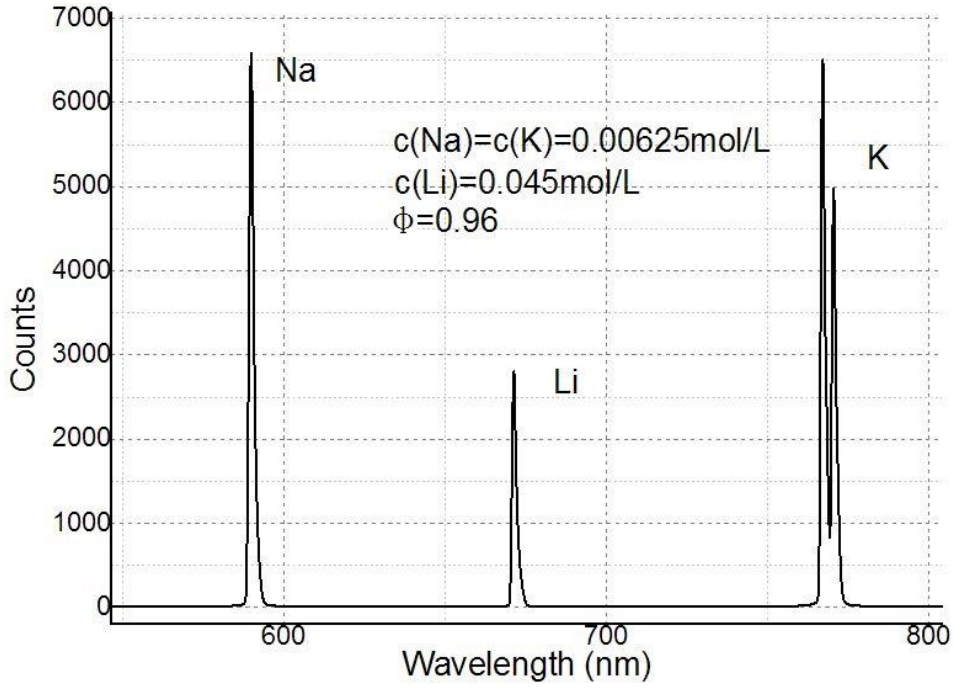

Figure 12: A typical emission spectrum with background subtraction

A typical alkali seeded flame emission spectrum of interested wavelength range is shown in Figure 12. The fluorescence signal was gathered five times under the same working condition (ϕ =1.23, c(Li)=0.027mol/L, c(Na)=c(K)=0.005mol/L) to obtain the stability properties of the system. The flame was quenched after each measurement. The interval between each ignition was 10 minutes, and the data were collected 3 minutes after each ignition.

The integral fluorescence signal counts in each measurement are shown in Table 4. The relative range of the measuring system is about 4%. This deviation mainly comes from the instability of the flame itself and the seeding system. The capillary tube used for alkali seeding is not stationary and thus may get shifted during the measuring process. The shift of the capillary opening will affect the pressure and thus slightly affect the seeding rate. The detection efficiency of the spectrometer is assumed to be constant and seldom affect the stability of the measuring system.

Table 4: The measured stability properties of the system

No.	Na	Li	K	$Na \cdot Li/K^2$	Na/K
1	30549	21337	63764	0.16032	0.47910
2	29543	20754	63075	0.15412	0.46837
3	28915	20479	61796	0.15506	0.46790
4	28827	20453	61205	0.15739	0.47098
5	28730	19880	61775	0.14967	0.46507
Average	29313	20581	62323	0.15531	0.47029
Standard deviation	680.63	473.34	945.48	0.003543	0.0047879
Relative range	4.2%	3.7%	2.3%	3.2%	1.9%

5.2 Fluorescence intensity dependence of the alkali concentration

The fluorescence intensities of sodium and potassium at various alkali concentrations were measured to obtain the optical operating concentration and signal-to-noise ratio (SNR). The results are shown in double logarithmic coordinate in Figure 13. The fluorescence intensities are on the increase and not saturated in the concentration range from 0.001mol/L to 1mol/L. The SNRs were observed by naked-eye and regard as high enough over the measured alkali concentration range. To reduce the self-absorption of the emitted light, solutions with lower concentration were selected for further measurement as shown in Table 3.

5.3 Temperature dependence of the fluorescence intensity ratio Na/K

The fluorescence intensities under various alkali solution concentrations and different equivalence ratios were measured. The ratio of measured sodium over potassium fluorescence intensity is given as a function of equivalence ratio in Figure 14 (a). The curves show similar

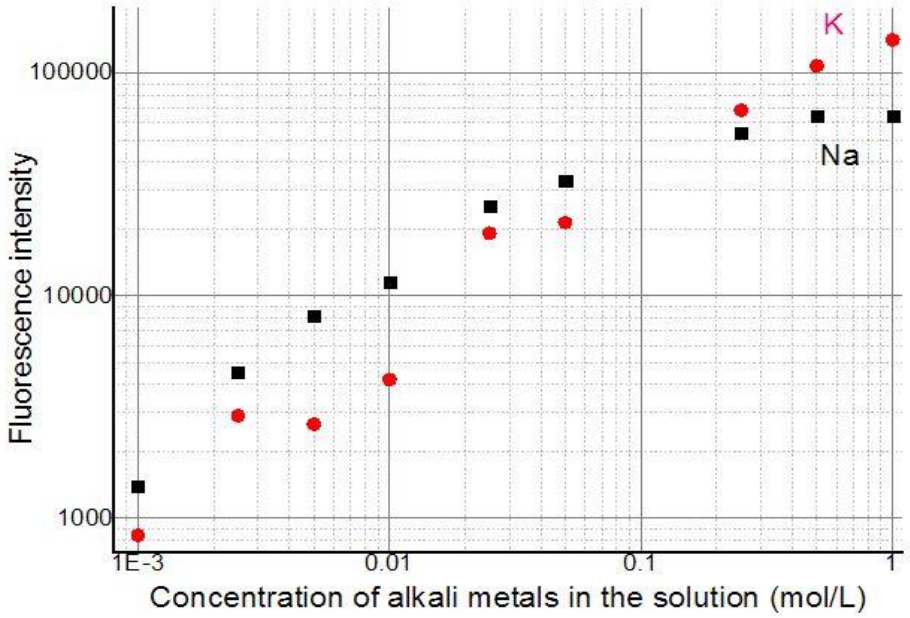

Figure 13: Fluorescence intensity as a function of the alkali concentration in the solution.

decline trend at the nearly stoichiometric ratio and fuel-rich zone. For the context of sodium and potassium concentration less than 0.025mol/L, the fluorescence intensity ratios are almost identical and not dependent on the specific alkali concentration, which does not correspond to the model simulation.

The temperature was measured under each operation condition; however, it turns out that temperatures are almost identical under different alkali concentrations and depend mainly on the equivalence ratio under the operating condition. The mean value shown in Table 5 was used in the following temperature dependence measurements within an error of 10 K at 1700K.

Table 5: The mean value of measured temperatures under each equivalence ratio

ϕ	0.85	0.96	1.04	1.14	1.23
T	1611.8	1671.2	1640.2	1611.8	1619.4

The relationship between the fluorescence intensity ratio and the gas temperature is thus obtained as shown in Figure 14 (b). The gas temperature at ϕ =0.85 and ϕ =1.14 are equivalent according to measurement, whereas the fluorescence intensity ratios are totally distinct. Because more data were collected in the range of fuel-rich, data collected at ϕ =1.14 are used in the figure of temperature dependence. Data collected at ϕ =0.85 were discarded, and more data are needed for the research of lean operating condition.

It can be seen that the ratio measured at the temperature around 1700 K is also much higher than expect (Figure 7). The measured Na/K fluorescence ratio is pretty sensitive to the temperature, although it does not coincide well with the prediction. It should be mentioned that no calibration measurement has been conducted for the thermocouple thermometer used in the lab, so the measured temperatures are not strictly precise. Moreover, other possible theoretical reasons and experimental errors such as the affection of chemiluminescence and the sensitivity of the spectrometer at different wavelength will be discussed in 5.5.

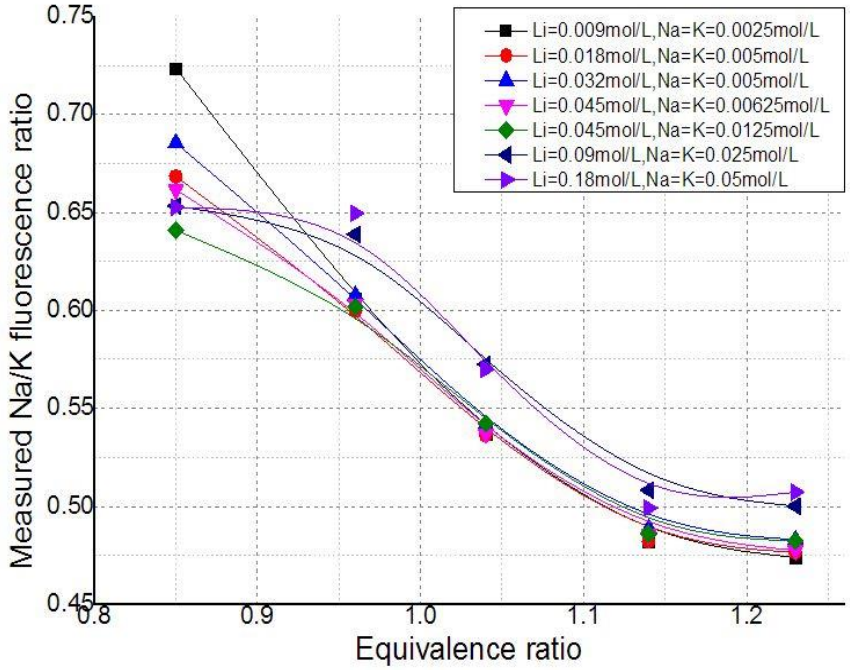

Figure 14(a): Measured Na/K fluorescence ratio over a range of alkali concentration as a function of equivalence ratio.

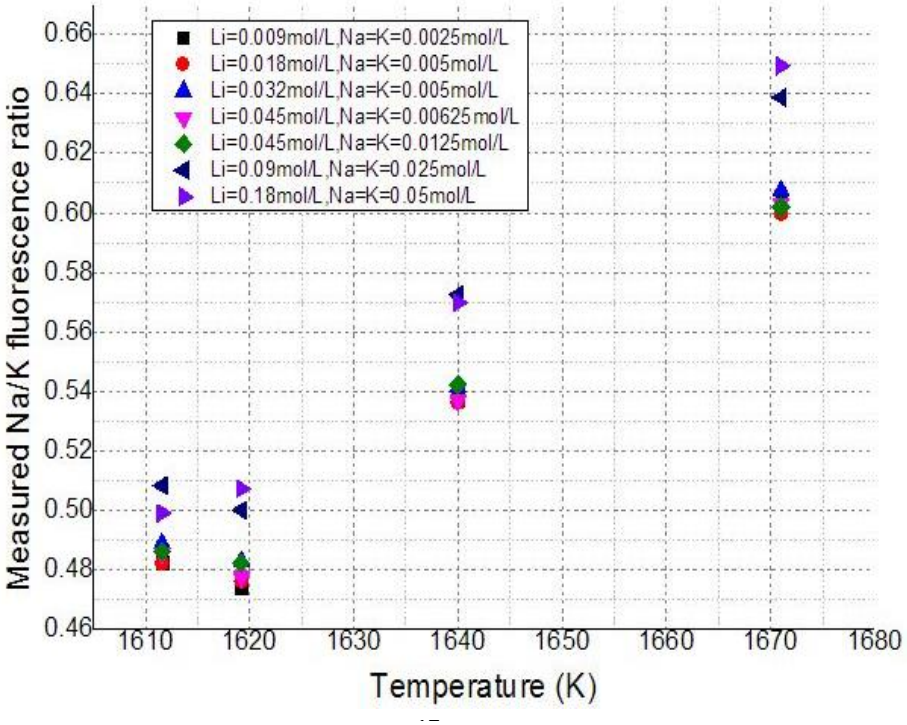

Figure 14(b): Measured Na/K fluorescence ratio over a range of alkali concentration as a function of measured temperature.

5.4 Temperature dependence of the fluorescence intensity ratio $\mathbf{Na \cdot Li/K^2}$

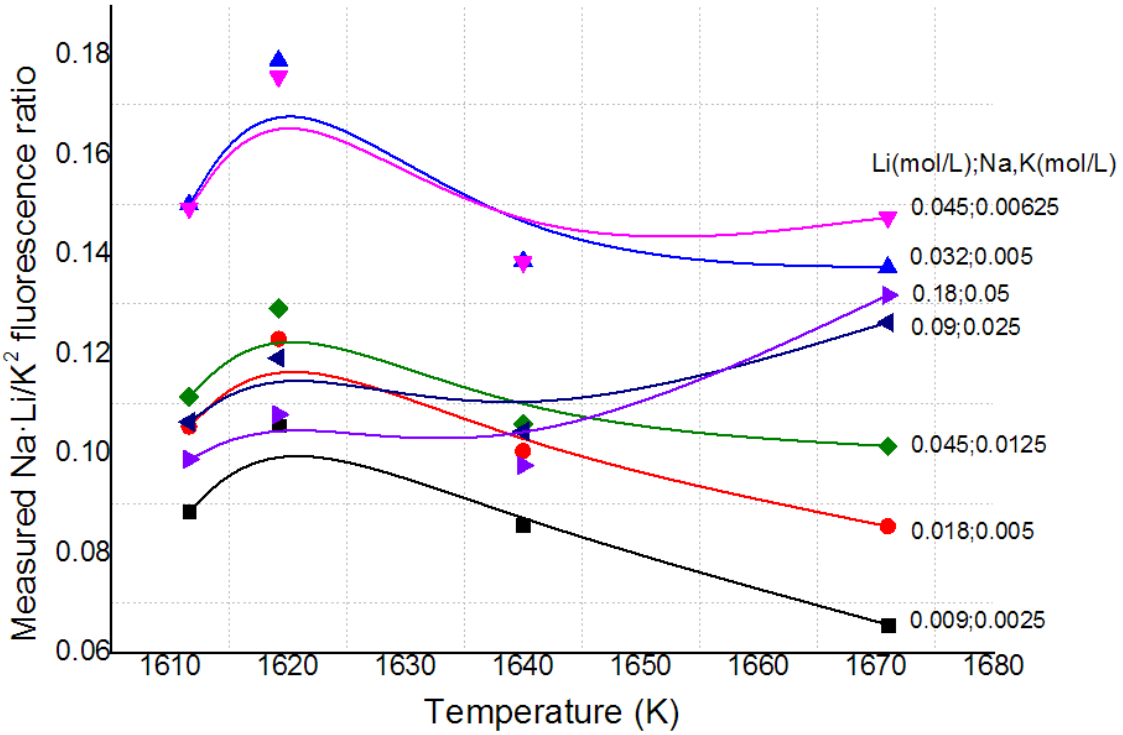

Figure 15: Measured Na·Li/K^2 fluorescence ratio as a function of temperature under various alkali concentrations.

Figure 15 shows the temperature dependence of measured Na·Li/K^2 fluorescence ratios. The concentration ratios of lithium over sodium and potassium are set to be constant for the lower five curves. The curve shows a different tendency when the concentration of sodium potassium is higher than 0.0125 mol/L, which is similar to the case of Na/K fluorescence ratio. A nearly parallel tendency can be seen observaing the curves with Na concentration lower than 0.025 mol/L, which is not strictly increasing or decreasing. Moreover, the fluorescence ratio Na·Li/K^2 is less temperature sensitive as it varies only 0.04 utmost for each fixed concentration over the temperature range of 60 K, making it improper for using as a temperature marker under the working conditions.

5.5 Discussion on deficiencies of the method

The primary deficiency of the model is the neglect of non-thermal radiation occurred in the flame, that is, chemiluminescence. In the FES method, almost all of the excitation energy ultimately comes from chemical reactions. Part of the heat transferred indirectly to the atoms in the process of inelastic collision and hence excites the atoms. The energy released in a particular chemical reaction can be converted directly to excitation energy which is in the context of chemiluminescence [24]. The energy released by chemical reactions in the flame is of the similar order of magnitude as the energy needed for atomic excitation energy. The energy of chemical reaction does not have to be identical to the excitation energy for the reason that any

possible excesses or insufficiencies of the energy can be compensated for simply by additional exchanges of kinetic energy.

Chemiluminescence deviates the fluorescence profile from thermal radiation only when the flame radicals relevant to the chemiluminescent reaction are not in chemical equilibrium, whereas suprathermal radiation has to be considered if the reactant concentration exceeds the equilibrium values. Suprathermal chemiluminescence radiation affects the alkali fluorescence intensity in two ways. On one hand, the concentration of the free atoms in the flame appreciably increased due to the strong reduction of the metal oxides caused by chemiluminescence effect. On the other hand, the fluorescence of metal atoms with excitation energies smaller than 5 eV is influenced by one of the two fundamental types of chemiluminescence of atomic lines, which is the so-called suprathermal chemiluminescence of the first kind [25]. This effect comes from the recombination reactions of free radicals H and OH which are in excess in the flame. The energy of recombination reaction brings about excitations. The metal atoms do not play a role in the recombination reaction itself but present as a non-active 'third body' as shown below:

$$H + H + M \rightarrow H_2 + M^*$$

and

$$H + OH + M \rightarrow H_2O + M^*$$

where M and M* are a non-excited and an excited metal atom respectively. In the case of the sodium doublet with Eq = 2.1 eV, the aforesaid effect appears only in cool flames with the temperature less than 1800 K. The burner used in the lab is water-cooled and thus meet the former condition.

Another problem is that the experiments were conducted at an atmosphere pressure, where the pressure is not high enough, so the assumption of thermal and chemical equilibria might be inaccurate.

Furthermore, the measured fluorescence intensity ratios are almost 3-4 times of the prediction, which may come from the different detection efficiency of the spectrometer at different wavelength. The signal intensity ratio can be largely affected if the spectrometer is much more sensitive around the wavelength of sodium than that of potassium. Besides, the mole fraction of alkali in the fuel was just a roughly estimate value due to the measuring error caused by the liquid residues in the connecting tube in the measurement of the alkali solution mass seeded into the flame. The seeding rate is influenced by the height of liquid level and the position of the capillary opening. Therefore, those are also factors that influence the fluorescence intensity.

6 Conclusion and Outlook

Preliminary experiments have been done to obtain the appropriate working conditions. The temperature dependence of excited state population, atomic mole fraction and self-absorption were plotted independently. The theoretical model for the temperature dependence of fluorescence intensity ratio Na/K in the case of thermal radiation in burned gas region was simulated for the operating condition.

The emitted fluorescence ratios Na/K measured is strongly temperature dependent and under the working condition with an atmosphere pressure and temperature ranged from 1600 K to 1700K. Although certain temperature dependency can be seen, it does not coincide well with the prediction. Theoretical deficiencies and measuring errors are discussed accordingly. The Na-Li/K[2] fluorescence ratio measured is shown to be less temperature sensitive and not suitable for using as a temperature marker in the operating temperature range.

More researches are required for the temperature dependence measurement. A theoretical model combined with the affection of thermal radiation and non-thermal radiation can be established to obtain a better consequence. A novel multi-jet burner designed by Wubin Weng et al. [26] that can provide hot flue gases with controlled gas compositions and temperature can be used in the future temperature dependence measurements to make the measurements more convenient and achieve a higher experimental accuracy. The concentration of the atomic Na, Li, and K in the hot gases can be measured directly by AAS to eliminate the error in both the seeding mass measurement and the calculation of thermodynamic equilibria. Further experiments can be conducted to measure the concentration of the excited and non-excited alkali metal atom in hot flue gases and obtained the excited state population directly.

Acknowledgements

There are many I would like to thank for their dedication and support to make this project possible. My supervisor Dr. Zhongshan Li, for giving me the opportunity to take on this project, for his guidance, patience and for showing and teaching me much more than the project alone encompassed. My co-supervisor Dr. Wubin Weng, for his endless help during the preparation and lab, helpful discussions, and for patient explanations to all of my questions. Thanks also go to my counsellor in Fudan University, Dr. Di Lu, for recommending this wonderful exchange program, and for the encouragement and inspiration all the time. I wish to thank all my friends in Lund for all the fun time and happy memories we have during this year.

References

1. Withrow, L. & Rassweiler, G. M. 1938. Studying engine combustion by physical methods - A review. Journal of Applied Physics, 9, 362-372.
2. G.M. RASSWEILER, L. WITHROW & W. CORNELIUS, SAE J. Trans. 46(1),25 (1940)
3. J. Reissing, J.M. Kech, K. Mayer, J. Gindele, H.Kubach & U.Spicher, SAE 1999-01-3688 (1999)
4. K.W.Beck, T.Heidenreich, S. Busch & U. Spicher, SAE 2009-32-0030 /20097030 (2009)
5. Mosburger, M., Sick, & V. Drake, M. C. 2013. Quantitative high-speed burned gas temperature measurements in internal combustion engines using sodium and potassium fluorescence. *Applied Physics B-Lasers and Optics*, 110, 381-396.
6. Mosburger, M., Sick, & V. Drake, M. C. 2014. Quantitative high-speed imaging of burned gas temperature and equivalence ratio in internal combustion engines using alkali metal fluorescence. *International Journal of Engine Research*, 15, 282-297.
7. Mosburger, M. J. 2013. Alkali metal spectroscopy for high-speed imaging of burned gas temperature, equivalence ratio and mass fraction burned in internal combustion engines. Doctor of Philosophy, The University of Michigan.
8. Bransden, B. H. & Joachain, C. J. 2003. *Physics of atoms and molecules*, Harlow, England ; New York, Prentice Hall.
9. "NIST Atomic Spectra Database", National Institute of Standards and Technology, https://www.nist.gov/pml/atomic-spectra-database, April 25, 2017.
10. H. P. Hooymayers & P. L. Lijnse, "The relationship between the fluorescence yield and the underpopulation of doublet excited states", J. Quant. Spectrosc. Radiat. Transfer 9, p.995 (1968).
11. D. R. Jenkins, "The determination of cross sections for the quenching of resonance radiation of metal atoms. I. Experimental method and results for sodium.", Proc. Roy. Soc. A 293 (1435), p.493 (1966).
12. I. R. Hurle, "Line reversal studies of the sodium excitation process behind shock waves in N2", J. Chem. Phys. 41, p.3911 (1964).
13. P. J. T. Zeegers & C. T. J. Alkemade, "Radical recombination in acetylene-air flames", Combustion and Flames 9, p.247 (1965).
14. W. E. Kaskan, "The reaction of alkali atoms in lean flames", 10th Symposium (International) on Combustion (1), p.41 (1965).

15. E. M. Bulewicz, C. G. James & T. M. Sugden, "Photometric investigations of alkali metals in hydrogen flame gases. II. The study of excess concentrations of hydrogen atoms in burnt gas mixtures", Proc. Roy. Soc. London A 235 (1200)(1956).
16. C. G. James & T. M. Sugden, "Photometric investigation of alkali metals in hydrogen flame gases. I. A general survey of the use of resonance radiation in the measurement of atomic concentrations", Proc. Roy. Soc. London A 227 (1170)(1955).
17. A. J. Hynes, M. Steinberg & K. Schofield, "The chemical kinetics and thermodynamics of sodium species in oxygen-rich hydrogen flames", J. Chem. Phys. 80 (6), p.2585 (1983).
18. Chemkin-pro 15131, Reaction Design: San Diego, 2013
19. A. L. Boers, C. T. J. Alkemade & J. A. Smit, "The yield of resonance fluorescence of Na in a flame", Physica XXII, p.358 (1956)
20. C. T. J. Alkemade, T. Hollander, W. Snelleman & P. J. T. Zeegers, Metal Vapor in Flames (Pergamon Press, 1982), ISBN 0-08-018061-2
21. Wolfram Research, Inc., Mathematica, Version 11.1, Champaign, IL (2017).
22. Leffler, T. 2016. Development and Application of Optical Diagnostics of Alkali Vapours for Solid Fuel Combustion. Doctor of Philosophy, Lund University.
23. Origin Version 9.0 (OriginLab, Northampton, MA)
24. Alkemade, C. T. J. & Herrmann, R. 1979. Fundamentals of analytical flame spectroscopy, New York, Wiley.
25. Bulewicz, E. M. & Padley, P. J. 1961. Suggested Origin of the Anomalous Line-Reversal Temperatures in the Reaction Zone of Hydrocarbon Flames. Combustion and Flame, 5, 331-340.
26. Weng, W., Borggren, J., LI, B., Aldén, M. & LI, Z. 2017. A novel multi-jet burner for hot flue gases of wide range of temperatures and compositions for optical diagnostics of solid fuels gasification/combustion. Review of Scientific Instruments, 88, 045104.

Appendices

Appendix A: Code used in the calculation of self-absorption (Potassium)

```
P:= {...} (*pressure in[Pa]*)
T:= {...} (*burned gas temperature in[K]*)
xK := {...} (*atomic mole fraction calculated by Chemikin-Pro*)

lmax:= 2.3 (*Maxium absorption length in[cm]*)
v0K:= 2.998*10^8/(766.5*10^-9)
AK:=3.8*10^7(*Einstein-A coefficient*)
fK:= AK*1.5*2*(766.5*10^-7)^2 (*K oscillator strength*)
nK:= xK* 273.15/(22.4*T)*6.023*10^23/1000 (*total number density of K atoms in burned gas after chemistry correction *)
mK:= 39.0983/(6.022*10^23)/1000 (*mass of K atom*)
mN:= 28/(6.022*10^23)/1000 (*mass of nitrogen molecule*)

QcK[P_, T_] := (P/(8.314*T))*6.022*10^23*188*10^-20*
  Sqrt[8*1.3806503*10^-23*
    T/3.14159*(1/mK + 1/mN)] (*collision rate of K with N2*)

vDK[T_, mK_, v0K_] := 2*Sqrt[2*Log[2]*1.3806503*10^-23*T/mK]*v0K/(2.998*10^8) (*Doppler broadened line width*)

vLK[AsK_, QcK_] := (AsK/(2*3.1416)) + (QcK/(2*3.1416)) (*Lorentz broadened line width *)

vVK[vDK_, vLK_] := 1/2*vLK +Sqrt[1/4*vLK^2+vDK^2](*Voigt broadened line width*)

SVK[vDK_, vLK_, v0K_, vK_, y_] := ((2*Sqrt[Log[2]])/(3.1416*Sqrt[3.1416]))*0.84*(vLK/
    vDK^2)*(Exp[-y^2]/((0.84*
          vLK/vDK)^2 + (((vK - v0K)*2*Sqrt[Log[2]])/vDK -
          y)^2)) (*Voigt broadened line profile*)

SVKint[vDK_, vLK_, v0K_] :=
 NIntegrate[(2*Sqrt[Log[2]])/(3.1416*Sqrt[3.1416])*0.84*vLK/vDK^2*
   Exp[-y^2]/((0.84*vLK/vDK)^2 + (((vK - v0K)*2*Sqrt[Log[2]])/vDK -
         y)^2), {vK, v0K - (1/1000*v0K),
   v0K + (1/1000*v0K)}, {y, -Infinity,
   Infinity}]
```

```
SVKint[vDK[T[[1]], mK, v0K], vLK[AsK, QcK[P[[1]], T[[1]]]], v0K] (*check if it integrates
to 1*)

kK[SK_, fK] := 2.65*10^-2*SK*fK (*spectral absorptivity of K*)

AbsK[SVK_, kK_, nK_, vVK_, lmax_] :=
 NIntegrate[ SVK/lmax*(1 - Exp[-kK*l*nK]), {vK, v0K - 10*vVK, v0K + 10*vVK}, {l,
   0, lmax}, {y, -Infinity,      Infinity}] (*fraction of reabsorbed K fluorescence*)

For[i = 1, i < imax + 1, i++,
 Print[AbsK[
   SVK[vDK[T[[i]], mK, v0K], vLK[AsK, QcK[P[[i]], T[[i]]]], v0K, vK,
    y], kK[SVK[vDK[T[[i]], mK, v0K], vLK[AsK, QcK[P[[i]], T[[i]]]],
     v0K, vK, y], fK], nK[[i]],
   vVK[vDK[T[[i]], mK, v0K], vLK[AsK, QcK[P[[i]], T[[i]]]]],
   lmax]]] (*Calculate for all P,T,n in array*)
```

Appendix B: Photographs of Experimental Setup

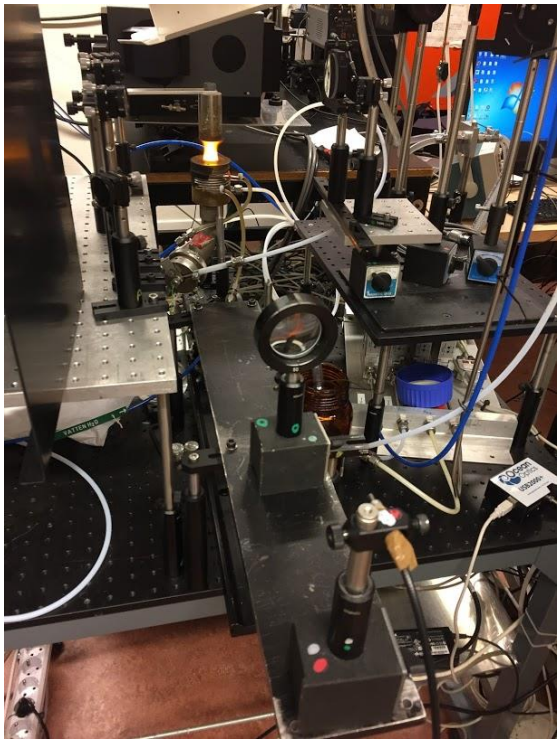

Figure 16: Top view of the experimental setup.

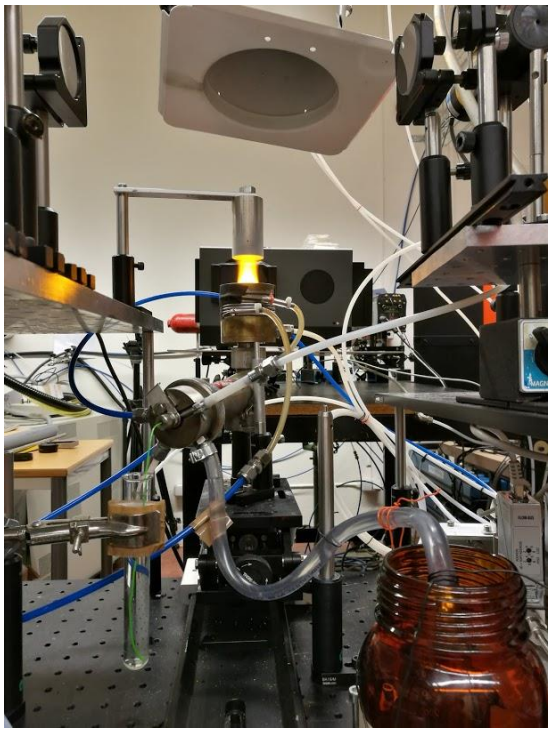

Figure 17: Side view of the experimental setup.
The test tube was replaced by a beaker due to the evident affection on the fluorescence measurement caused by the liquid level.